EBioMedicine 67 (2021) 103355

Contents lists available at ScienceDirect

EBioMedicine

journal homepage: www.elsevier.com/locate/ebiom

Article

Increased viral variants in children and young adults with impaired humoral immunity and persistent SARS-CoV-2 infection: A consecutive case series

Thao T. Truong[a], Alex Ryutov[a], Utsav Pandey[b], Rebecca Yee[a], Lior Goldberg[c,d], Deepa Bhojwani[c,d], Paibel Aguayo-Hiraldo[c,d,i], Benjamin A. Pinsky[e,f], Andrew Pekosz[g], Lishuang Shen[a], Scott D. Boyd[e,j], Oliver F. Wirz[e], Katharina Röltgen[e], Moiz Bootwalla[a], Dennis T. Maglinte[a], Dejerianne Ostrow[a], David Ruble[a], Jennifer H. Han[a], Jaclyn A. Biegel[a,d], Maggie Li[g], ChunHong Huang[e], Malaya K. Sahoo[e], Pia S. Pannaraj[d,h], Maurice O'Gorman[a,d], Alexander R. Judkins[a,d], Xiaowu Gai[a,d], Jennifer Dien Bard[a,d,*]

[a] Department of Pathology and Laboratory Medicine, Children's Hospital Los Angeles, Los Angeles, CA, United States
[b] Department of Pathology, Westchester Medical Center/New York Medical College, Valhalla, NY, United States
[c] Department of Pediatrics, Cancer and Blood Disease Institute, Division of Hematology-Oncology, Children's Hospital Los Angeles, Los Angeles, CA, United States
[d] Keck School of Medicine, University of Southern California, Los Angeles, CA, United States
[e] Department of Pathology, Stanford University School of Medicine, Stanford, CA, United States
[f] Division of Infectious Diseases and Geographic Medicine, Department of Medicine, Stanford University School of Medicine, Stanford, CA, United States
[g] W. Harry Feinstone Department of Molecular Microbiology and Immunology, Johns Hopkins Bloomberg School of Public Health, Baltimore, MD, United States
[h] Department of Pediatrics, Division of Infectious Diseases, Children's Hospital Los Angeles, Los Angeles, CA, United States
[i] Department of Pediatrics, Cancer and Blood Disorder Institute, Transplant and Cellular Therapy Section, Children's Hospital Los Angeles, CA, United States
[j] Sean N. Parker Center for Allergy and Asthma Research, Stanford, CA, United States

ARTICLE INFO

Article History:
Received 4 February 2021
Revised 22 March 2021
Accepted 8 April 2021
Available online xxx

Keywords:
SARS-CoV-2
immunocompromised
persistent infection
variants
case report
pediatric

ABSTRACT

Background: There is increasing concern that persistent infection of SARS-CoV-2 within immunocompromised hosts could serve as a reservoir for mutation accumulation and subsequent emergence of novel strains with the potential to evade immune responses.
Methods: We describe three patients with acute lymphoblastic leukemia who were persistently positive for SARS-CoV-2 by real-time polymerase chain reaction. Viral viability from longitudinally-collected specimens was assessed. Whole-genome sequencing and serological studies were performed to measure viral evolution and evidence of immune escape.
Findings: We found compelling evidence of ongoing replication and infectivity for up to 162 days from initial positive by subgenomic RNA, single-stranded RNA, and viral culture analysis. Our results reveal a broad spectrum of infectivity, host immune responses, and accumulation of mutations, some with the potential for immune escape.
Interpretation: Our results highlight the potential need to reassess infection control precautions in the management and care of immunocompromised patients. Routine surveillance of mutations and evaluation of their potential impact on viral transmission and immune escape should be considered.

1. Introduction

Infection with severe acute respiratory syndrome coronavirus-2 (SARS-CoV-2), the cause of coronavirus disease 2019 (COVID-19) is most commonly detected using reverse transcription polymerase chain reaction (RT-PCR). Viral load typically peaks with onset of symptoms and wanes to undetectable levels by week three, when patients generally begin to develop antibodies [1]. While the Centers for Disease Control and Prevention (CDC) recommends quarantining for 14 days following exposure to COVID-19, the time course of infection may vary due to factors including age, immune status, and disease severity [2]. In most patients, culture, contact tracing, and subgenomic RNA detection studies have not demonstrated infectivity

* Corresponding author at: Department of Pathology and Laboratory Medicine, Children's Hospital Los Angeles, Los Angeles, CA, United States.
E-mail address: jdienbard@chla.usc.edu (J.D. Bard).

https://doi.org/10.1016/j.ebiom.2021.103355

Research in context

Evidence before this study

There has been substantial interest in the phenomenon of prolonged shedding of SARS-CoV-2. Although an increasing number of case reports have described the course of disease in immunocompromised individuals, definitive evidence for prolonged active replication with infectious virus and corresponding immunological data has been scarce. We searched PubMed, bioRxiv, and medrxiv for these reports using the terms "immunocompromised," "immunosuppressed," "SARS-CoV-2," "replication," "shedding," and "infectivity" for relevant articles published up until December 26, 2020. We found four articles that have utilized longitudinal sequencing, detection of subgenomic RNA, and/or viral culture to demonstrate ongoing infectivity in immunocompromised adults.

Added value of this study

Our study presents a more complete picture of the spectrum of prolonged infection for up to 162 days, which is the longest reported to-date, in three immunocompromised patients using viral culture, detection of both subgenomic and single-stranded RNA, whole-genome sequencing, and characterization of host serological responses. Secondly, this is the first report, to our knowledge, characterizing prolonged infection in pediatric and young adult patients. Thirdly, we demonstrated the clear presence of intra-host viral heterogeneity as evidence of ongoing viral evolution within the hosts. We note two of our patients acquired several mutations in the gene encoding the spike protein at specific residues that may be important for antibody binding. Finally, we present a potential correlation between the host immune response and the emergence of mutations in the spike gene.

Implications of all the available evidence

Given recent interest in the emergence of a potentially more transmissible variant of SARS-CoV-2, there is a need to better understand the dynamics of within-host accumulation of mutations in immunocompromised hosts, whether or not they remain infectious, if these mutations could mediate immune escape, and what kind of immunological selection pressures may drive such mutations. Altogether, these findings have important public health implications for infection control precautions and management in this patient population.

beyond 10 days of symptom onset [3,4]. In rare cases prolonged shedding of SARS-CoV-2 has been observed in immunocompromised adults, making study of this population critically important [5–8]. However, the temporal dynamics of SARS-CoV-2 infectivity and the evolution of SARS-CoV-2 mutational profiles over prolonged periods of infection in immunocompromised patients, particularly in children, have not been described. Beyond the implications for individual patients, the emergence of B.1.1.7 SARS-CoV-2 and other lineages with potential for immune evasion has led to greater focus on the importance of genomic surveillance [9,10]. Here, we describe prolonged SARS-CoV-2 RT-PCR positivity in two children and one young adult undergoing therapy for B-cell acute lymphoblastic leukemia (ALL). In addition to evidence of ongoing replication, two of these cases demonstrated significant intra-host SARS-CoV-2 mutational accumulation and host immune responses that may have contributed to their disease course.

2. Methods

2.1. Case histories

Patient 1 is a previously healthy 3-year-old female with no significant past medical history prior to several admissions to the emergency department (ED) for worsening pancytopenia, decreased appetite, and abdominal pain. Her bone marrow biopsy revealed 58% blasts consistent with B-cell ALL and a chemotherapy regimen was initiated (Fig. 1A, Table 1). Asymptomatic screening for SARS-CoV-2 by RT-PCR at time of discharge revealed a positive result (day 0). She was re-admitted to the hospital on day 3 for fatigue and vomiting as well as cough, malaise, and gastrointestinal symptoms and discharged on day 6. She consistently tested positive for SARS-CoV-2 during follow-up screens for her chemotherapy until she finally tested negative on day 91 without any notable respiratory symptoms (Fig. 1A, Fig. 2A).

Patient 2 is a 21-year-old male who was previously diagnosed with B-cell ALL six months prior to his first SARS-CoV-2 positive RT-PCR. He received combination chemotherapy, however continued to have detectable residual disease at the end of the consolidation phase, prompting initation of CD19-directed chimeric antigen receptor T cell therapy (CAR-T, Tisagenlecleucel, Cassiopeia protocol). He had prolonged pancytopenia including B-cell aplasia after CAR-T infusion. Upon a follow up visit to the transplant and cell therapy clinic 3 weeks after infusion, the patient was tested for SARS-CoV-2 due to concerns for possible contact exposure and was positive (day 0). On day 6 after the initial positive test he presented to the ED with decreased appetite, fever, and two days of dry cough. His chest x-ray showed a diffuse interstitial prominence and a small bilateral pleural effusion. He developed intermittent fevers with increased oxygen requirement over the next several days, including an episode of acute hypoxemic respiratory failure necessitating 10 liters of oxygen via face mask on day 18. He received a 5-day course of Remdesivir. From then on his oxygen requirement was weaned down to 2-3 liters via nasal cannula (NC), however he continued to have intermittent fevers and bilateral patchy ground glass opacities on chest CT. He improved after a second 5-day course of Remdesivir, weaned down off supplemental O2 to his nighttime baseline of 0.5L/NC while asleep (used to treat his mild obstructive sleep apnea) and was discharged on day 45. He was hospitalized four additional times for persistent fevers with negative infectious work-up except for a persistently positive SARS-CoV-2 RT-PCR with consistently high (Ct range: 17.2 – 28.1) viral loads. Weekly convalescent plasma therapy was initiated on day 103 and changed to every other week beginning day 144. Unfortunately on day 156, he developed worsening cough, new fevers, and was found to be hypoxemic down to 80% needing supplemental oxygen with 4L/NC. Full infectious disease workup failed to demonstrate any additional infection besides persistently positive SARS-CoV-2 RT-PCR. He was admitted to the hospital and received convalescent plasma. Thereafter, he resumed weekly convalescent plasma infusions. His anti-SARS-CoV-2 IgG was finally positive on day 103 which was likely due to the plasma infusion initiated that day prior to antibody measurement. He has remained SARS-CoV-2 RT-PCR positive through his most recent test on day 250 at the time of this publication.

Patient 3 is a 2-year-old male who was diagnosed with high-risk B-cell ALL 7 months prior to presentation to the ED with fever and confirmed positive for SARS-CoV-2 upon admission (day 0). At admission he demonstrated tachycardia and pancytopenia that were attributed to his chemotherapy. After clinical improvement, he was discharged on day 6 but re-admitted on day 14 with recurrent fever and tachycardia. He continued to be febrile, had worsening pancytopenia likely related to chemotherapy, pulmonary infiltrates, and increasing oxygen requirements to 5L via face mask by day 32, at which time he received a 5-day regimen of Remdesivir. His fevers and respiratory distress improved and he was discharged on day 40, only to be readmitted for fever on day 43 and discharged on day 51.

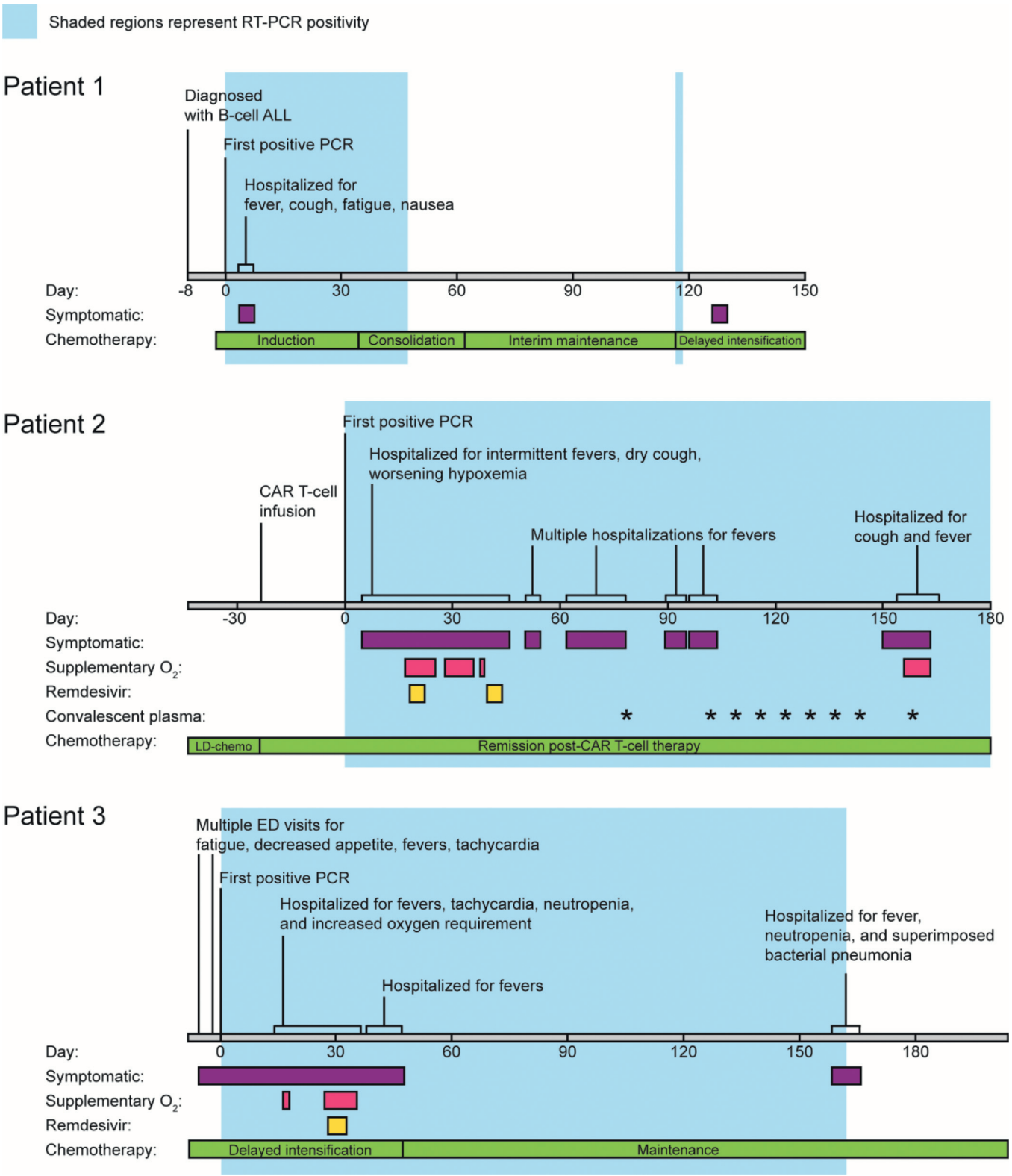

Fig. 1. Clinical timeline.

Timelines of symptoms, hospital admissions, and treatment for patient 1, patient 2, and patient 3 are labelled by date from initial positive RT-PCR (day 0). Colored bars indicate time periods where patients were symptomatic, required supplementary oxygen, or received treatment (Remdesivir or convalescent plasma). The phases of chemotherapy are also shown. ED, emergency department; LD-chemo, lymphodepleting-chemotherapy.

The patient then started maintenance chemotherapy. Anti-SARS-CoV-2 IgG was repeatedly negative or borderline and finally became positive on day 83. He was re-admitted on day 162 for possible urinary tract infection and subsequently developed tachypnea, fever, and cytopenia. Chest CT scans on days 47, 96, and 166 showed persistent multifocal pneumonia and scattered areas of ground-glass and consolidative opacities, with shifting opacities that increased in some areas but improved in others. He improved on antibiotics and was discharged on resolution of his fevers on day 173. He was last RT-PCR positive on day 162 and finally negative on day 196. A

Table 1
Demographic, oncological, and clinical characteristics of study patients.

	Patient 1	Patient 2	Patient 3
Demographic characteristics			
Age (years)	3	21	2
Sex	Female	Male	Male
Oncological characteristics			
Oncological diagnosis	SR B-ALL	HR B-ALL, refractory	HR B-ALL
Other coexisting medical conditions	None	Obstructive sleep apnea Hypothyroidism Intermittent Asthma	None
Oncological treatment	Chemotherapy	Lymphodepleting chemotherapy and CAR-T cell therapy	Chemotherapy
Phases of oncological treatment during viral shedding	-Induction -Consolidation -Interim maintenance -Delayed intensification	Post- CAR-T cell therapy	-Delayed intensification -Maintenance
Active immunosuppressive or immunomodulatory drugs at time of initial SARS-CoV-2 detection	SR B-ALL chemotherapy per COG AALL0932: Dexamethasone, vincristine, peg-asparaginase, methotrexate, 6-MP, doxorubicin	Cyclophosphamide and Fludarabine as lymphodepleting agents prior to CAR-T cell therapy	HR B-ALL chemotherapy per COG AALL0232: Cyclophosphamide, cytarabine, thioguanine, vincristine, dexamethasone, methotrexate, mercaptopurine
Chemotherapy	Yes (detailed above)	Yes (detailed above)	Yes (detailed above)
Corticosteroids	Yes (per chemotherapy protocol)	No	Yes (per chemotherapy protocol)
CAR-T therapy	No	Yes, Tisagenlecleucel	No
Clinical, laboratory and imaging data			
Days of PCR positivity	46 (inconclusive/positive again day 116-117)	165+ from time of report	162
Symptomatic at time of initial positivity	No	No	Yes
Symptomatic at any positive time point	Yes	Yes	Yes
Symptoms			
Fever	Yes	Yes	Yes
Malaise	Yes	Yes	Yes
Cough	Yes	Yes	Yes
Sore throat	Yes	No	Yes
Headache	No	No	No
Shortness of breath	No	Yes	Yes
Congestion/rhinorrhea	No	Yes	Yes
Vomiting	Yes	Yes	Yes
Abdominal pain	Yes	Yes	Yes
Anosmia and Ageusia	Unable to assess	Unable to assess	Unable to assess
Other infectious disease findings	No	- *Clostridioides difficile* diarrhea - *Staphylococcus hominis* bacteremia (day +7)	Superimposed bacterial pneumonia (day 162, improved with antibiotics)
Laboratory data at initial positivity	WBC: 2.14 K/μL ANC: 0.74 K/μL ALC: 1.36 K/μL	WBC: 2.30 K/μL ANC: 1.59 K/μL ALC: 0.42 K/μL	WBC: 0.65 K/μL ANC: 0.00 K/μL ALC: 0.56 K/μL
Lymphocyte subsets	Not done	Day +7 to +158 (multiple) CD3: 75-1000 cells/μL CD4: 31-314 cells/μL CD8: 52-747 cells/μL CD19: $<$1 cell/μL throughout	Day +13 CD3: 1204 cells/μL CD4: 194 cells/μL CD8: 987 cells/μL CD19: 1 cells/μL
Chest CT scan	Not done	Bilateral patchy ground glass opacities involving all lobes, predominantly peripherally in lower lobes (similar in all 3 CT scans on days +38, +73 and +116)	Persistent multifocal pneumonia and scattered areas of ground-glass opacities, with shifting opacities increased in some areas but improved in others (CT scans on days +22, +47, +96, +166)
Treatment for COVID-19 infection			
Oxygen supplementation	No	Yes, intermittent (total of 22 days above baseline with maximal 10L per minute via facemask)	Yes (total of 11 days above with maximal 5L per minute via facemask)
COVID-19 related ICU admissions	No	Yes (5 days)	No
Mechanical ventilation	No	No	No
Remdesivir	No	Yes, two 5 day courses	Yes, one 5 day course
Convalescent plasma	No	Yes (measured as ratio serum to calibrator absorbance) Day 78: 4.3 Day 103: 9.1 Day 110: 8.6 Day 123: 8.3 Day 130: 7.5 Day 137: 4.6 Day 144: 1.4 Day 158: 4.1 Day 165: 3.4 Day 172: 1.53	No

SR, standard risk; HR, high risk; B-ALL, B-cell acute lymphocytic leukemia; CAR-T, chimeric antigen receptor T-cell therapy; COG, Children's Oncology Group; WBC, white blood cells; ANC, absolute neutrophil count; ALC, absolute lymphocyte count; CT, computerized tomography; ICU, intensive care unit.

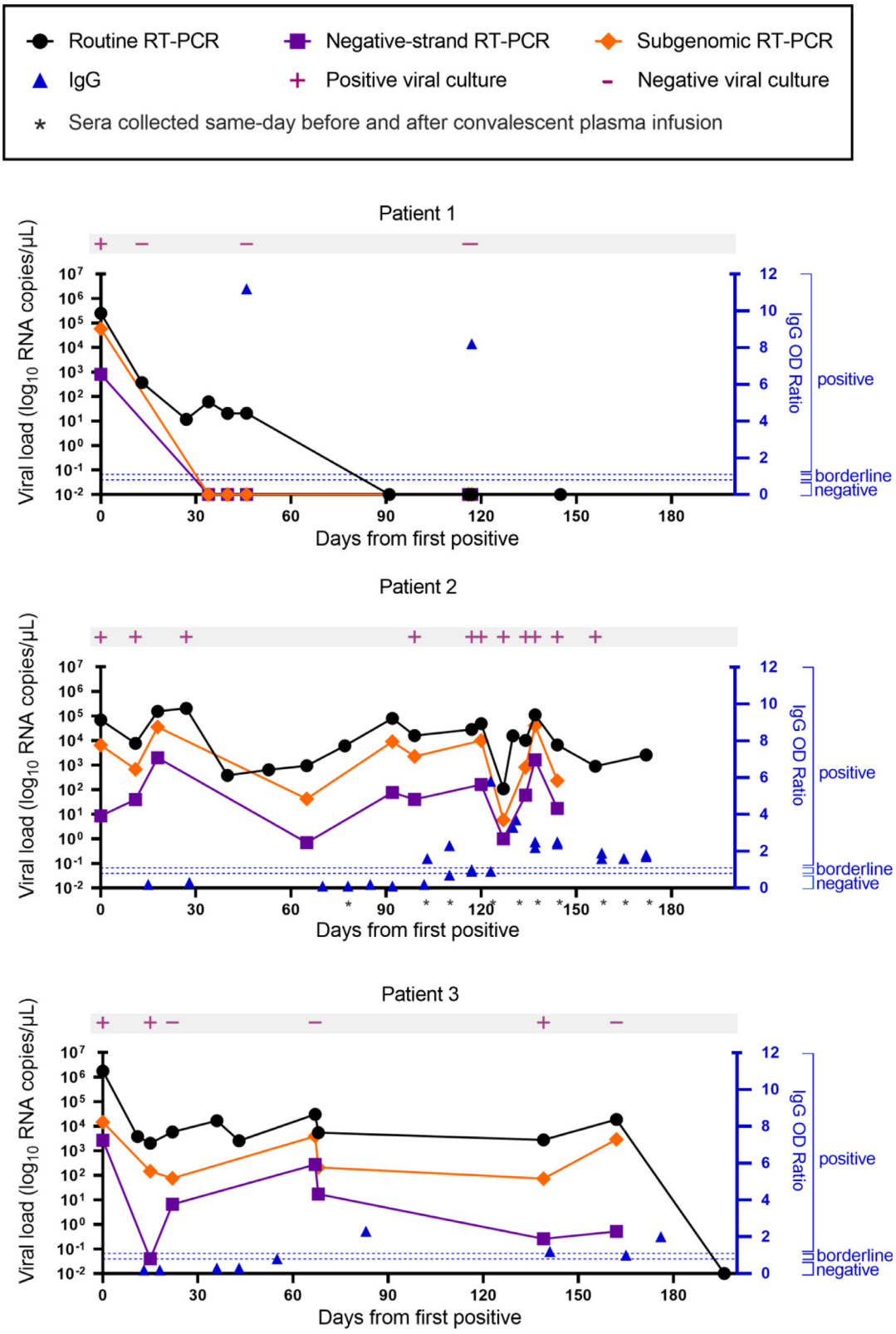

Fig. 2. SARS-CoV-2 Viral load by method.

Time course of viral load by routine, negative-strand, and subgenomic RT-PCR from nasopharyngeal or combined nares/oropharyngeal swabs collected from each patient. Viral culture results are indicated in pink. Corresponding serum anti-SARS-CoV-2 IgG values are plotted in blue. For patient 2, IgG was measured before and after administration of convalescent plasma at the indicated timepoints.

surveillance chest CT scan on day 230 showed near complete resolution of his pulmonary disease.

2.2. Ethics

The study was approved by the CHLA Institutional Review Board (CHLA-16-00429) as part of a large multi-center study and the study was granted a waiver of informed consent/assent/permission per CGR 46.116(d). In addition, verbal consent/assent was obtained from all three patients.

2.3. Study cohort

All patients presenting to the Hematology-Oncology department at Children's Hospital Los Angeles (CHLA) between May 7 to November 21, 2020 who were repeatedly SARS-CoV-2 positive by RT-PCR for at least 40 days with cycle threshold (Ct) consistently $\leq$31 were considered for this consecutive case series. Specimens from all three patients meeting these criteria were obtained at CHLA between May 7 to November 21, 2020 for clinical testing for various indications including hospital admissions both related and unrelated to COVID-19, asymptomatic pre-procedural screening, evaluation of COVID-19 related and unrelated symptoms, and after a high-risk exposure to someone with confirmed SARS-CoV-2 infection. Disease severity was categorized using Centers for Disease Control and Prevention's classification as previously described [11].

2.4. Data analysis

Patient demographics, clinical course and management data were obtained from the hospital electronic medical record (EMR). Specimens were coded and all research staff were blinded to all specimen identity and collection timepoint throughout the sequencing, viral culture, strand-specific, subgenomic, and serological assays. No statistical analyses were performed.

2.5. Detection of SARS-CoV-2 RNA

Nasopharyngeal swabs or combined oropharyngeal and nares swabs were sent to the Clinical Virology Laboratory at CHLA for testing. The molecular assays used were the CDC 2019-Novel Coronavirus Real-Time RT-PCR assay, the Taqpath COVID-19 RT-PCR assay (Thermo Fisher, Walham, MA), the Xpert Xpress SARS-CoV-2 assay (Cepheid, Sunnyvale, CA), and the Simplexa COVID-19 assay (Diasorin Molecular, Cypress, CA). Total nucleic acid was extracted according to manufacturer's instructions as outlined in the respective Emergency Use Authorization [11–14]. Viral loads (copies/mL) were calculated based on a standard curve generated by testing samples with known viral copy numbers for each assay as previously described [11].

2.6. Viral culture

Viral culture was performed using SARS-CoV-2-susceptible VeroE6TMPRSS2 cells[15,16] adapted from the VeroE6 cell line (ATCC CRL-1586) to express the TMPRSS2 protease at levels approximately 10-fold higher than that found in the human lung. 150 μL of clinical specimen was used to inoculate one well of a 24 well plate of VeroE6TMPRSS2 cells as previously described [15,17]. After a 2-hour incubation at 37°C, the inoculum was removed and replaced with 0.5 ml infection media and the plates incubated at 37°C for 5 days. The plates were scored daily for cytopathic effect and supernatants harvested when >75% of the cells had detached. The presence of SARS-CoV-2 viruses in the harvested supernatants was then verified by quantitative RT-PCR using the CDC N1 and RNase P primer sets on RNA extracted with the viral RNA isolation kit (Qiagen, Germantown, MD).

2.7. Quantitative two-step strand-specific SARS-CoV-2 RT-PCR

A two-step strand-specific SARS-CoV-2 RT-PCR assay targeting the *envelope* (E) gene was performed as previously described by Hogan et al. as a biomarker to predict presence of actively replicating virus [18]. In the first set of reactions, reverse transcription with strand-specific primers converts SARS-CoV-2 RNA to complementary DNA (cDNA). In the second step, the cDNA is amplified by real-time PCR in using the Rotor-Gene Q instrument (QIAGEN). A standard-curve to convert minus-strand Ct values to copies/μL was generated using *in vitro* transcribed minus-strand *E* gene RNA.

2.8. Subgenomic SARS-CoV-2 RT-PCR

One-step subgenomic (sg) SARS-CoV-2 RT-PCR utilizing a forward primer targeting the 5' leader sequence and reverse primer and probe complementary to *E* gene sequences was adapted from Wolfel et al. and combined in multiplex with the Hong Kong Orf1ab and Centers for Disease Control and Prevention RNAse P primer/probe sets [19,20]. as an additional biomarker for actively replicating virus. Real-time RT-PCR was performed using the Rotor-Gene Q instrument. A standard-curve to convert sgRNA Ct values to copies/μL was generated using *in vitro* transcribed plus-strand RNA encoding the leader and *E* gene sequences (Log_{10} copies/μL = -0.288*Ct + 11.351).

2.9. Measurement of anti-SARS-CoV-2 antibodies in serum

IgG to the S1 domain of SARS-CoV-2 spike was measured from serum within 24 hours of collection with a commercial enzyme-linked immunosorbent assay (ELISA) kit (EUROIMMUN, Lubeck, Germany) [21]. A ratio of sample to calibrator optical density of $<$ 0.8 is considered negative, $\geq$ 0.8 to $<$1.1 is considered borderline, and $\geq$1.1 is considered positive.

In addition, IgA, IgG and IgM to SARS-CoV-2 nucleocapsid (N) protein, spike S1, and receptor binding domain (RBD) and the competition ELISA procedure were measured as recently described by Röltgen et al. [22].

2.10. ELISA to detect anti-SARS-CoV-2 antibodies in serum samples

IgA, IgG and IgM to SARS-CoV-2 nucleocapsid (N) protein, spike S1, and receptor binding domain (RBD) and the were measured with a laboratory-developed ELISA as previously described by Röltgen et al. Briefly, 96-well Corning Costar high binding plates (Thermo Fisher) were coated with viral antigens at 0.1 μg per well (0.025 μg per well for the nucleocapsid IgG assay) overnight at 4°C. Serum or plasma samples were incubated in coated plates at a 1:100 dilution. Specific antibodies were detected with horseradish peroxidase conjugated goat anti-human IgG (γ-chain specific, catalog no. 62-8420, Thermo Fisher, 1:5,000 dilution), IgM (μ-chain specific, catalog no. A6907, Sigma, 1:5,000 dilution), or IgA (α-chain specific, catalog no. P0216, Agilent, 1:2,000 dilution). Plates were developed with 3,3′,5,5′-Tetramethylbenzidine (TMB) substrate and optical density (OD) at 450 nm was measured for sample wells with subtraction of blank well values. Seroconversion was defined as values above the mean plus three times the standard deviation of ELISA ODs from 94 pre-pandemic negative control samples from healthy blood donors. Control data were from non-immunocompromised COVID-19 patients less than 60 years old, sampled at least 50 days after symptom onset, and admitted to hospital without ICU care. All samples were tested twice in independent experiments.

2.11. Competition ELISA to detect antibodies that block binding of ACE2 to RBD

The competition ELISA was recently described in Röltgen et al. [22]. Briefly, RBD-coated ELISA plates were incubated with plasma

samples at a 1:10 dilution before addition of recombinant ACE2 expressed as a fusion protein with mouse IgG2a Fc (ACE2-mFc) at 0.5 μg/mL. Detection of RBD-ACE2-mFc was done with horseradish peroxidase conjugated goat anti-mouse IgG (Fc specific, catalog no. 31439, Invitrogen, 1:10,000 dilution), developed and measured as described aboce. Two quality controls (Access SARS-CoV-2 IgG QC, QC1-QC2, 2 levels, catalog no. C58964, Beckman Coulter) were included on each plate. OD values were converted to percentage of RBD-ACE2 blocking using the following formula: percentage blocking = 100*(1-(sample OD - 0.2)/(QC1 OD − 0.2)), taking into account the background noise of the assay of 0.2 which was determined by testing historical negative control serum samples. All samples were tested three times in independent experiments.

2.12. AmpliSeq multiplex-PCR method and S5XL sequencing

Confirmatory SARS-CoV-2 sequencing using the AmpliSeq SARS-CoV-2 Research Panel was done for viral samples with lower viral loads (Table S4). Viral RNA amplification and library preparation was performed according to the manufacturer's protocol using the Ion AmpliSeq Library Kit Plus (Thermo Fisher Scientific) and two pools of custom primers. cDNA was synthesized using SuperScript VILO cDNA Synthesis Kit (SuperScript IV), in either 15 μL or 6 μL reactions using 9.6 or 4.8μL of RNA combined with 2.4 or 1.2 μL (respectively) of 5X VILO IV Master Mix (an additional 3μL of nuclease-free water was added to the 15 μL reactions); larger cDNA reactions were used for automated library prep on Ion Chef (Thermo Fisher Scientific) and the smaller volume reaction for manual library preparation. The reaction was incubated at 25°C for 10 minutes, 50°C for 10 minutes, and 85°C for 5 minutes. Following cDNA conversion, for manual library prep, separate multiplexed PCR reactions were set up for primer pool 1 and 2 using half of the cDNA for each primer pool, 2 μL of 5X Ion AmpliSeq HiFi Mix, 2 μL of 5X Ion AmpliSeq SARS-CoV-2 Research Panel primer pool 1 or 2, and nuclease-free water for a total volume of 10 μL per primer pool. PCR conditions used were as follows: initial activation of enzyme at 99°C for 2 minutes, 16-26 cycles of denaturation (99°C for 15 seconds) and annealing/extension (60°C for 4 minutes), and hold at 10°C. Primer pool 1 and 2 target amplification reactions were combined and partial digestion of amplicons and barcode ligation carried out according to the manufacturer's protocol. The barcoded libraries then were purified using 1X beads-to-sample ratio of Agencourt AMPure XP Magnetic Beads and 70% Ethanol. The libraries were quantified using the Ion Library TaqMan Quantitation Kit and diluted to 30 pmol/L and pooled together. For Ion Chef automated library preparation, primer pools were diluted to 2x and added to the reagent cartridge; reagents, consumables, and cDNA in an Ion-Code PCR plate were loaded into the Ion Chef instrument per the Ion AmpliSeq on Chef protocol. A total of 16-27 cycles of amplification were performed for libraries generated on Chef with an anneal/extension time of 4 minutes. Final library pools generated by the Chef were quantified using the Ion Library TaqMan Quantitation Kit and normalized to 30 pmol/L.

A total of 25 μL of the pooled libraries was loaded onto the Ion Chef System for automated clonal amplification by emulsion PCR using Ion 510, 520/530 Chef Reagents and consumables and subsequent chip loading (520 or 530 chips). Viral genome sequencing was performed on the Ion Torrent S5 XL platform using standard 200-base sequencing chemistry.

2.13. TWIST target-capture method and Illumina sequencing

Confirmatory SARS-CoV-2 sequencing using the Twist SARS-CoV-2 Research Panel was done for viral samples with higher viral loads (Table S4). cDNA libraries were generated using Twist Library Preparation Kit for ssRNA Virus Detection. cDNA was generated per the Twist SARSCoV2-Virus Detection Protocol by annealing 5 μL Random Primer 6 (New England Biolabs) to up to 15 μL of RNA and incubating the 20 μL reaction volume at 95°C for 5 minutes; 25 μL of ProtoScript II Reaction Mix and 5 μL of ProtoScript II Enzyme Mix (New England Biolabs) were added to the primer annealed RNA for first strand synthesis (25°C for 5 minutes, 42°C for 60 minutes, and 80°C for 5 minutes). The NEBNext Ultra II Non-Directional RNA Second Strand Synthesis Module (New England Biolabs) was used to create second strand cDNA per the Twist protocol, and the cDNA was purified using SPRI Beads (Beckman Coulter Life Sciences). cDNA (enzymatic) fragmentation, end repair, and dA-tailing were carried out using the Twist Library Preparation EF Kit (Twist Bioscience) to generate TruSeq-compatible libraries. Universal adapters (Twist Biosciences) were ligated to libraries, and libraries were purified and subsequently amplified using Twist UDI primers and Kapa HiFi HotStart Ready Mix (Roche). A total of 12 cycles of amplification were used (98°C for 45 seconds, followed by 12 cycles of 98°C for 15 seconds, 60°C for 30 seconds, 72°C for 30 seconds, and a final extension of 72°C for 1 minute, and final hold at 4°C). Finally, the amplified, indexed libraries were purified and quantified using the Promega QuantiFluor ONE dsDNA System. A total of 1,500ng of each amplified product was hybridized to the Twist SARS-CoV-2 probe mix for 15 minutes at 60°C following the Twist protocol. Capture was performed using Twist binding beads and the Twist Fast Hybridization and Wash kit per the kit protocol. Captured libraries were amplified for 15 cycles (98°C for 45 seconds, followed by 15 cycles of 98°C for 15 seconds, 60°C for 30 seconds, 72°C for 30 seconds, and a final extension of 72°C for 1 minute, and final hold at 4°C). Amplified libraries were purified before library fragment profiles were quantified using the Agilent 4200 TapeStation High Sensitivity DNA assay. Library concentrations were normalized to ~5nM and pooled to a final pool concentration of 4nM then denatured and diluted according to the Illumina MiSeq Denature and Dilute Libraries Guide and loaded on the sequencer at 10pM. Paired-end and dual-indexed 2 × 150bp sequencing was done using Micro Kit v2 (300 Cycles).

2.14. Consensus genome comparison, phylogenetic analysis and clade analysis

Consensus genomes obtained on the patient isolates were compared to the Wuhan isolate (NC_045512.2) using SARS-CoV-2 Genome App v1.1 (https://cov2annot.cpmbiodev.net) and CHLA COVID-19 Analysis Research Database (CARD) to identify synonymous, non-synonymous and intergenic variations [23,24]. Phylogenetic analysis and evolutionary rate estimation were performed using packages available through Nextstrain command-line interface (v 2.0.0.) [25]. Consensus viral sequences for each patient were combined to generate a multiple sequence alignment with MAFFT (version 7.460) using speed-oriented option - FFT-NS-i (iterative refinement method, two cycles) optimized for large datasets [26]. A maximum likelihood tree using Bayesian information criteria was generated with IQ-TREE (version 2.0.3) using GTR substitution model [27]. The resulting rate estimation and phylogeny was then time-resolved using TreeTime (version 0.7.6) and visualized using auspice [25,28]. Phylogenetic clade analysis was performed using Nextclade (version 0.3.7).

2.15. Viral genome library construction and sequencing

Whole-genome sequencing (WGS) libraries of viral cDNA were prepared as previously described using the CleanPlex SARS-CoV-2 Research and Surveillance NGS Panel (Paragon Genomics, Hayward, CA) [11]. Libraries were then quantified and normalized to approximately 7nM and pooled to a final concentration of 4nM; libraries were denatured and diluted according to Illumina protocols and loaded on the MiSeq at 10pM. Paired-end and dual-indexed 2 × 150bp sequencing was done using Micro Kit v2 (300 Cycles).

Libraries yielding average depth ≥ 1000x were considered high quality and used for downstream analysis, and variant calling was performed for nucleotide positions with ≥100x coverage.

2.16. Genome assembly and variant calling

Coverage profiles, variant calls and consensus genomes were generated using the in-house software system LUBA (Lightweight Utilities for Bioinformatics Analysis) [11]. Ion Torrent aligner TMAP (Thermo Fisher) was used to generate AmpliSeq BAMs. Sequencing of majority of clinical specimens by two alternate methods were also pursued to validate Paragon variant calls (appendix p 1-3). Paragon and Twist nucleotide sequences were aligned with NovoAlign (Novocraft Technologies, Selengor, Malaysia) aligner. Ion Torrent aligner TMAP (Thermo Fisher) was used to generate AmpliSeq BAMs.

2.17. Role of the funding source

The funders had no role in study design, data collection, data analysis, data interpretation, or writing of the report. The corresponding author had full access to all the data in the study and had final responsibility for the decision to submit for publication.

3. Results

3.1. Viral detection by RT-PCR and culture

Specimens from all three patients were collected and used to detect SARS-CoV-2 RNA over the course of 6 months. In addition to viral culture, we performed strand-specific and subgenomic RT-PCR to detect ongoing replication [4,18,19]. The viral load in patient 1 was highest at day 0 and then gradually declined and was last reliably detected on day 46 (Fig. 2A). Culturable virus was only detected in the day 0 sample and subsequent cultures were negative. The SARS-CoV-2 minus strand and subgenomic RNA was only detected from the first sample taken on day 0 and not in any subsequent samples (Fig. 2A).

The viral load in patient 2 remained consistent through day 172 despite two courses of Remdesivir and weekly administration of convalescent plasma. Consistent with these results, SARS-CoV-2 was recovered by viral culture for up to day 144. Viral cultures were not explored past 144 days from initial positive. Strikingly, the minus strand and subgenomic RNA was detected in nearly all of the samples from patient 2 and the Ct values trended with the corresponding viral load (Fig. 2B).

Patient 3 also maintained consistent viral loads through day 162 despite weak seroconversion on day 83, and finally tested negative on day 196 (Fig. 2C). He demonstrated variable viral recovery with positive cultures from days 0, 22, and 139, and negative cultures from days 15, 67, and 162 which we believe reflects poor sample integrity or a transient reduction in infectious virus production given that subgenomic and minus strand RNA was readily detectable up through day 162.

3.2. Antibody response

We assessed each patient's serological response profile using ELISAs to measure IgA, IgG, and IgM antibodies specific to the SARS-CoV-2 receptor binding domain (RBD), S1, and N proteins. Patient 1 had a strong IgA, IgG, and IgM response to all tested antigens at days 46 and 117, consistent with their more typical clinical course of infection and recovery, with viral RNA not reliably detected after day 46 (Fig. 3A). In contrast, patient 2, who had culturable virus up to day 144 and positive viral RNA up to day 172, was more weakly IgG positive and was negative for IgA and IgM to all tested SARS-CoV-2 antigens from days 110-144 (Fig. 3B). Importantly, paired sera obtained from patient 2 before and after convalescent plasma infusion showed increased IgG levels after infusion which were rapidly waning. As this patient had B-cell aplasia following CAR T-cell therapy, his ability to mount an immune response was impaired. Patient 3 had detectable viral RNA at least up to day 162, and showed serological results spanning days 83-176 with a weakly positive IgG and unusually high levels of IgM for the RBD, S1, and Spike proteins, but negative N antibodies (Fig. 3C). Antibody levels were compared to four non-immunocompromised COVID-19 patients, who showed the typical increase of anti-SARS-CoV-2 IgG, IgM, and IgA antibodies between one to two weeks after symptom onset. IgA and IgM antibody levels began to wane about 3 to 4 weeks after symptom onset, while IgG levels were more stable (Fig. 3D).

We also measured the ability of the patients' sera to interfere with the interaction between the RBD of the SARS-CoV-2 spike protein and the angiotensin-converting enzyme 2 (ACE2) receptor *in vitro* (Fig. 3E). Sera from patient 1 from days 46 and 117 achieved 100% blocking, whereas patient 2's sera only weakly blocked the ACE2-RBD interaction on day 123 post-infusion and the other timepoints failed to block the interaction. Samples from patient 3 from days 83, 141, and 176 also showed poor blocking activity (Fig. 3E). Plasma samples from the four control patients showed varying degrees of RBD-ACE2 blocking activity. In a previous study higher RBD-ACE2 blocking percentages were correlated with higher anti-RBD antibody levels[22]. The antibody results were overall consistent with what we observed from the blocking assay, with the strongest immune response in patient 1, least effective response in patient 2, and a weak response in patient 3.

3.3. Genomic sequencing analysis

Specimens from patient 1 showed only a single major allele variant difference between days 0 and 27. Decreasing viral load precluded sequencing of specimens from later timepoints. Patients 2 and 3 demonstrated an increase in intra-host viral diversity over time in variants of both high (major) and low (minor) allele frequencies across the viral genome (Fig. 4). In patient 2, 3 major allele variants emerged between days 0 and 40 with an additional 4 major and 7 minor allele variants by day 144. In patient 3, 13 major and 8 minor allele variants emerged by day 162. Virus clade predictions did not change across the specimens from each patient (patients 1 and 3: clade 20C and patient 2: clade 20A), providing further support that these patients were continuously infected rather than reinfected. Of particular note was the emergence of several spike gene mutations including 3 inframe deletions at residues S:Δ141-143, S:Δ145, and S:Δ141-144, a deletion-insertion at S:Δ211-212, and several nonsynonymous mutations including N440K, V483A, and E484Q at residues that have independently mutated in other lineages (Fig. 4, appendix p 6-12). Sequencing of additional library preparations by two alternate methods confirmed the variant calls (appendix p 1-3).

4. Discussion

We report two pediatric and one young adult patient with B-cell ALL with remarkably different courses of SARS-CoV-2 infection. Patient 1 had milder symptoms with rapidly declining and nonviable virus and serological evidence of a robust immune response that is representative of a typical COVID-19 clinical course [1]. By contrast, patients 2 and 3 experienced more severe COVID-19 characterized by serological evidence of a weaker immune response with evidence of prolonged infectious virus shedding and mutation accumulation demonstrating emergence of potential escape mutations.

The infection control implications suggest it is important to closely monitor immunocompromised patients who are persistently positive by SARS-CoV-2 RT-PCR and to determine whether or not the virus is actively replicating for a prolonged period of time. Using RT-

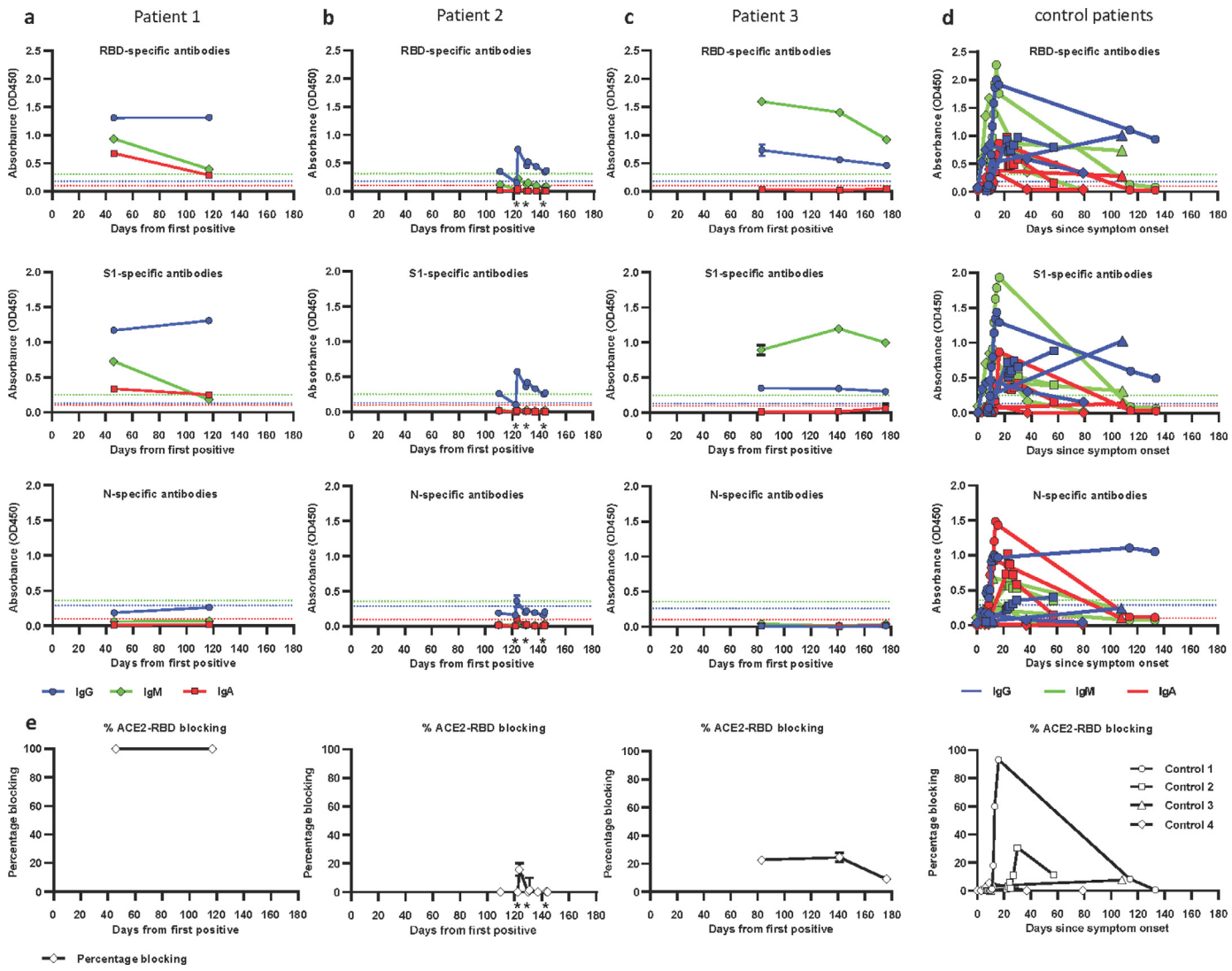

Fig. 3. Anti-SARS-CoV-2 antibody responses.

Serum samples from two immunocompromised children (a, c) and one young adult (b) were collected up to 176 days after initial positive SARS-CoV-2 PCR test. Plasma samples from four non-immunocompromised COVID-19 patients were analyzed for comparison (d). Antibodies specific for SARS-CoV-2 Spike RBD (top row), S1 subunit (second row), and N protein (third row) were measured. RBD-ACE2 blocking activity was assessed in a competition ELISA and is shown as percentage of blocking (e). The cutoff for seropositivity was defined as the mean absorbance + 3 SD of 94 historical negative serum samples in each assay. Color coding for isotypes: IgG (blue), IgM (green), IgA (red). Dotted lines depict the cut-off for seroconversion for the different isotypes in each assay. Individual donors were shown with different symbols (d). * indicates timepoints of convalescent plasma infusion in patient 2. Values are means ± 1 standard deviation for experimental triplicates.

PCR to detect subgenomic and negative-strand replication intermediates, we were able to identify ongoing replication throughout the samples from patient 2 (up to 144 days) and patient 3 (up to 162 days). It is notable that subgenomic RNA was readily detected for this length of time given that it is rarely detected past 8 days [4,5,19]. Overall the detection of viral intermediates correlated very well with the viral culture data, suggesting these may serve an expeditious molecular surrogate for infectivity. Viral culture was intermittently positive up to day 139 in patient 3. As culturing methods are limited by sample quality and lower sensitivity compared to molecular methods, it is more likely that the consistently positive results by subgenomic and negative-strand RT-PCR accurately represented continued replication within patient 3.

There has been considerable interest in the rapidly spreading SARS-CoV-2 B.1.1.7 variant due to its potential increased transmissibility. Relative to the SARS-CoV-2 reference sequence, B.1.1.7 has acquired 17 mutations, 8 of which are in the spike gene. There is concern that such a divergent variant could have emerged from long-term replication within an immunocompromised host, especially with the lack of closely related viral isolates [9]. Although we did not find these mutations in our patients, we did observe mutations in several regions within the spike gene. A V70P mutation appeared at day 162 in patient 3, overlapping the region where a S:Δ69-70del in the B.1.1.7 variant may enhance infectivity [29]. Several other observed mutations mapped to important residues in the spike gene. We observed emergence of a S:Δ141-144 and S:Δ145 deletion in patient 2 and a S:Δ141-143 deletion in patient 3. Similar mutations in this region of the spike gene have been found to abolish the binding of the anti-spike protein 4a8 blocking/neutralizing monoclonal antibody (Fig. 3, Tables S3-4) [7,30]. Additionally, in patient 3, N440K within the spike RBD emerged with an allele frequency of 0.51 on day 162 (Fig. 3, Table S4). This variant was also found by another group to confer antibody escape [31]. This mutation is adjacent to the position of a N439K variant of interest currently circulating in several lineages in Europe, which may enhance affinity of the binding of the spike protein to the ACE2 receptor and influences binding of monoclonal antibodies [32]. At day 139 the sequenced specimen from patient 3 also had mutations at V483A and E484Q within the RBD.

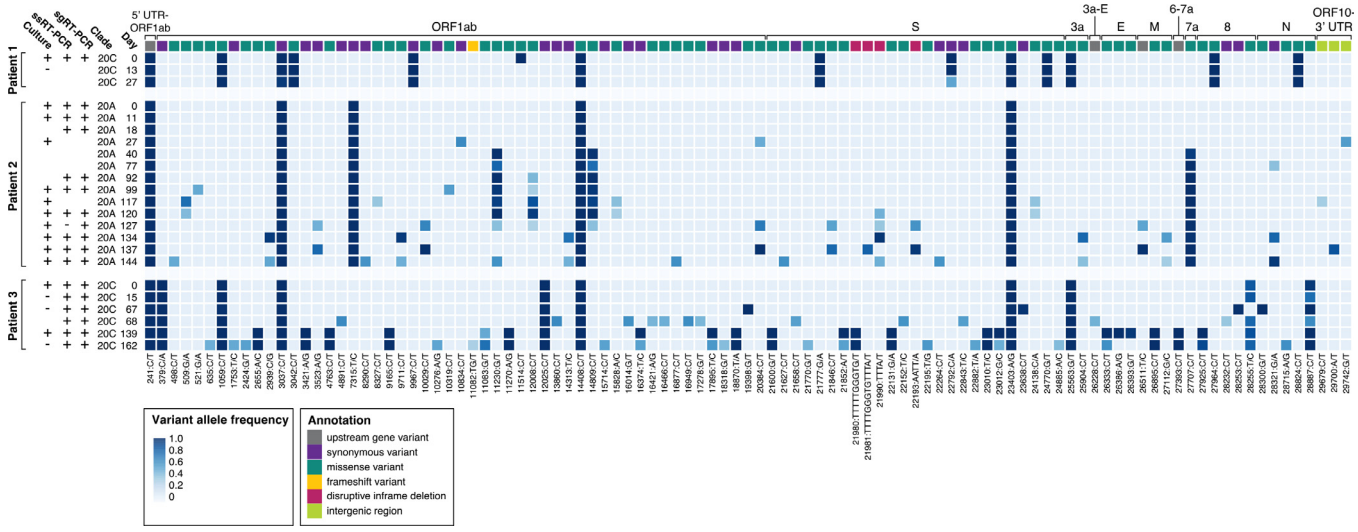

Fig. 4. Accumulation of SARS-CoV-2 variants.

Each row represents viral culture, strand-specific RT-PCR (ssRT-PCR), subgenomic RT-PCR (sgRT-PCR) and sequencing from longitudinally derived specimens numbered by days from initial positive test (day 0). Boxes represent distinct variants, and shading reflects variant allele frequency (cutoff = 0.25). Corresponding genes are labeled in top row and colored to represent variant annotation (see legend).

UTR, untranslated region; S, spike; E, envelope; M, matrix; N, nucleocapsid.

These residues were similarly associated with *in vitro* antibody binding and escape, and there has been interest in another mutation at the same position, E484K, which has emerged in the S.501Y.V2 lineage in South Africa (Fig. 3, Table S4) [31,33–35]. Similar mutations at these positions (N440D, E484A, and E484K) have independently arisen within other persistently infected, immunocompromised patients [5,7].

Analysis of patient antibody responses was performed to aid in understanding the persistent detection of SARS-CoV-2. Patient 1 was associated with very limited detection of active replication and had high levels of ACE2-RBD blocking antibodies, a surrogate measure of potential viral neutralizing antibodies *in vivo*. Patients 2 and 3 by contrast both had poor antibody responses, associated with evidence of prolonged infectivity. In immunocompetent patients, IgM, IgG, and IgA antibodies are generally detectable by day 20 post symptom onset [22]. Patient 3 had an atypical persistence of high IgM levels on days 83, 141, and 176 without evidence of evolution to IgG or IgA, suggestive of an impaired immune response perhaps related to his partially immunocompromised state. It is unlikely that the detection of IgM in this patient is related to infection with a new viral strain as the majority of the mutations that emerged in patient 3 are rarely found in the general population (Table S4). In general, all three patients had higher levels of antibodies targeting RBD and S1 compared to N, and this pattern has been previously observed in patients with milder illness compared to patients who died or were admitted to intensive care units [22]. However, compared to patients 1 and 2, patient 3 completely lacked antibodies to the N protein (Fig. 3C). It is possible that the spike-focused immune response, which weakly blocked ACE2, led to the emergence of escape mutants. There were more mutations in the spike gene, particularly in the RBD region, in patient 3 compared to patient 2 and many of these emerged on day 139 or 162, a time period where his antibody levels were rising. Patient 2 was treated with two courses of remdesivir and several infusions of convalescent plasma, however antibody levels waned rapidly after each infusion, possibly due to redistribution in the body or partial consumption and clearance. These treatments failed to control viral replication and did not apparently lead to as many mutations with the potential for immune escape as observed in patient 3. We note that anti-SARS-CoV-2 antibody levels start to decrease as soon as one month after symptom onset in some previously healthy COVID-19 patients, therefore it is possible that our measurements at later time points may underestimate the peak antibody levels acheived by patients 2 and 3 throughout their clinical course [22].

Our work demonstrates that immunocompromised pediatric and young adult patients are susceptible to prolonged viral infections with prolonged infectious virus shedding and mutation accumulation. The patients we report are immunocompromised to varying degrees, and our evidence suggests a potential correlation between host immune response and the emergence of viral variants, some of which may have the potential to escape antibody neutralization. We acknowledge the potential for selection bias in this small consecutive case series, who may not be wholly representative of the wider population of immunocompromised patients. Further work is needed to better understand the many host factors that can influence viral clearance and mutation within patients across a broader spectrum of immune deficiencies. However, we conclude that the observed expanded intra-host heterogeneity of viral isolates from pediatric and young adult patients with suppressed immunity and correspondingly prolonged infection raises the possibility of emergence of variants with the potential to evade immune responses elicited during the course of infection or induced by vaccine. This possibility warrants further study and, in the meantime, serious consideration of extended infection control precautions and genomic monitoring in this patient population.

Author Contributions

TT, XG, UP, RY, AR, and DB conceptualized the study. All authors contributed to data curation, investigation, and methodology. TT, AR, UP, and OW created the figures. TT, UP, RY, XG, and DB wrote the initial manuscript draft. TT, AR, UP, XG, and DB verified the underlying data. All authors reviewed and approved of the final manuscript.

Declaration of Competing Interests

S.D.B. has consulted for Regeneron, Sanofi, and Novartis on topics unrelated to this study. S.D.B., and K.R. have filed provisional patent applications related to serological tests for SARS-CoV-2 antibodies. All other authors have no competing interests.

Acknowledgments

The work was partially funded by The Saban Research Institute at Children's Hospital Los Angeles intramural support for COVID-19 Directed Research (X.G. and J.D.B.), the Johns Hopkins Center of Excellence in Influenza Research and Surveillance HHSN272201400007C (A.P.), NIH/NIAID R01AI127877 (S.D.B.), NIH/NIAID R01AI130398 (S.D.B.), NIH 1U54CA260517 (S.D.B.), an endowment to S.D.B. from the Crown Family Foundation, an Early Postdoc.Mobility Fellowship Stipend to O.F.W. from the Swiss National Science Foundation (SNSF), and a Coulter COVID-19 Rapid Response Award to S.D.B. L.G. is a SHARE Research Fellow in Pediatric Hematology-Oncology. The authors thank the ATUM Bio team for optimization, production, and sharing of antigens used in this study. We thank the National Institute of Infectious Diseases, Japan, for providing VeroE6TMPRSS2 cells.

Data availability

All genomic data were uploaded to GISAID. The corresponding accessions are available upon request from the corresponding author.

Funding

The work was partially funded by The Saban Research Institute at Children's Hospital Los Angeles intramural support for COVID-19 Directed Research (X.G. and J.D.B.), the Johns Hopkins Center of Excellence in Influenza Research and Surveillance HHSN272201400007C (A.P.), NIH/NIAID R01AI127877 (S.D.B.), NIH/NIAID R01AI130398 (S.D.B.), NIH 1U54CA260517 (S.D.B.), an endowment to S.D.B. from the Crown Family Foundation, an Early Postdoc.Mobility Fellowship Stipend to O.F.W. from the Swiss National Science Foundation (SNSF), and a Coulter COVID-19 Rapid Response Award to S.D.B. L.G. is a SHARE Research Fellow in Pediatric Hematology-Oncology.

Supplementary materials

Supplementary material associated with this article can be found, in the online version, at doi:10.1016/j.ebiom.2021.103355.

References

[1] Sethuraman N, Jeremiah SS, Ryo A. Interpreting Diagnostic Tests for SARS-CoV-2. JAMA 2020;323:2249.
[2] CDC. COVID-19 and Your Health. Centers for Disease Control and Prevention 2020 published online Feb 11 https://www.cdc.gov/coronavirus/2019-ncov/if-you-are-sick/quarantine.html. Accessed December 27, 2020.
[3] Walsh KA, Spillane S, Comber L, et al. The duration of infectiousness of individuals infected with SARS-CoV-2. J Infect 2020;0. doi: 10.1016/j.jinf.2020.10.009.
[4] Perera RAPM, Tso E, Tsang OTY, et al. SARS-CoV-2 virus culture and subgenomic RNA for respiratory specimens from patients with mild coronavirus disease - Volume 26, Number 11—November 2020 - Emerg Infect Dis J - CDC. DOI:10.3201/eid2611.203219.
[5] Avanzato VA, Matson MJ, Seifert SN, et al. Case Study: Prolonged infectious SARS-CoV-2 shedding from an asymptomatic immunocompromised cancer patient. Cell 2020 published online Nov 4. doi: 10.1016/j.cell.2020.10.049.
[6] Baang JH, Smith C, Mirabelli C, et al. Prolonged Severe Acute Respiratory Syndrome Coronavirus 2 Replication in an Immunocompromised Patient. *J Infect Dis* DOI:10.1093/infdis/jiaa666.
[7] Choi B, Choudhary MC, Regan J, et al. Persistence and Evolution of SARS-CoV-2 in an Immunocompromised Host. New England J Med 2020;0 null.
[8] Aydillo T, Gonzalez-Reiche AS, Aslam S, et al. Shedding of Viable SARS-CoV-2 after Immunosuppressive Therapy for Cancer. New England J Med 2020;0 null.
[9] Rambaut A, Loman N, Pybus O, et al. Preliminary genomic characterisation of an emergent SARS-CoV-2 lineage in the UK defined by a novel set of spike mutations. COVID-19 Genomics Consortium UK, 2020 https://virological.org/t/preliminary-genomic-characterisation-of-an-emergent-sars-cov-2-lineage-in-the-uk-defined-by-a-novel-set-of-spike-mutations/563 (Accessed 21 December 2020).
[10] Lineage-specific growth of SARS-CoV-2 B.1.1.7 during the English national lockdown. Virological 2020 published online Dec 30 https://virological.org/t/lineage-specific-growth-of-sars-cov-2-b-1-1-7-during-the-english-national-lockdown/575/1. Accessed December 31, 2020.
[11] Pandey U, Yee R, Shen L, et al. High Prevalence of SARS-CoV-2 Genetic Variation and D614G Mutation in Pediatric Patients with COVID-19. *Open Forum Infect Dis* DOI:10.1093/ofid/ofaa551.
[12] appliedbiosystems. TaqPath COVID-19 Combi Kit and TaqPath COVID-19 Combo Kit Advanced Instructions for Use. 2020; published online Nov 20. https://www.fda.gov/media/136112/download (Accessed 13 December, 2020).
[13] DiaSorin Molecular. Simplexa COVID-19 Direct. 2020; published online May 28. https://www.fda.gov/media/136286/download.
[14] Cepheid. Xpert Xpress SARS-CoV-2 Instructions for Use. 2020; published online Sept. https://www.fda.gov/media/136314/download (Accessed 13 December 2020).
[15] Gniazdowski V, Morris CP, Wohl S, et al. Repeat COVID-19 Molecular Testing: Correlation of SARS-CoV-2 Culture with Molecular Assays and Cycle Thresholds. Clin Infect Dis 2020 published online Oct 27. doi: 10.1093/cid/ciaa1616.
[16] Pekosz A, Parvu V, Li M, et al. Antigen-based testing but not real-time polymerase chain reaction correlates with severe acute respiratory syndrome coronavirus 2 viral culture. Clin Infect Dis 2021 published online Jan 20. doi: 10.1093/cid/ciaa1706.
[17] Pekosz A, Cooper CK, Parvu V, et al. Antigen-based testing but not real-time PCR correlates with SARS-CoV-2 virus culture. medRxiv 2020 : 2020.10.02.20205708.
[18] Hogan CA, Huang C, MK S, et al. Strand-specific reverse transcription PCR for detection of replicating SARS-CoV-2. Emerg Infect Dis 2021 published online Feb. doi: 10.3201/eid2702.204168.
[19] Wölfel R, Corman VM, Guggemos W, et al. Virological assessment of hospitalized patients with COVID-2019. Nature 2020;581:465–9.
[20] Chu DKW, Pan Y, Cheng SMS, et al. Molecular diagnosis of a novel coronavirus (2019-nCoV) causing an outbreak of pneumonia. Clin Chem 2020 published online Jan 31. doi: 10.1093/clinchem/hvaa029.
[21] Tilley K, Ayvazyan V, Martinez L, et al. A cross-sectional study examining the seroprevalence of severe acute respiratory syndrome coronavirus 2 antibodies in a university student population. J Adolesc Health 2020;67:763–8.
[22] Röltgen K, Powell AE, Wirz OF, et al. Defining the features and duration of antibody responses to SARS-CoV-2 infection associated with disease severity and outcome. Science Immunology 2020;5. doi: 10.1126/sciimmunol.abe0240.
[23] Zhu N, Zhang D, Wang W, et al. A Novel Coronavirus from Patients with Pneumonia in China, 2019. New England J Med 2020;382:727–33.
[24] Shen L, Maglinte D, Ostrow D, et al. Children's Hospital Los Angeles COVID-19 Analysis Research Database (CARD) - A Resource for Rapid SARS-CoV-2 Genome Identification Using Interactive Online Phylogenetic Tools. bioRxiv 2020 : 2020.05.11.089763.
[25] Hadfield J, Megill C, Bell SM, et al. Nextstrain: real-time tracking of pathogen evolution. Bioinformatics 2018;34:4121–3.
[26] Katoh K, Toh H. Recent developments in the MAFFT multiple sequence alignment program. Briefings in Bioinformatics 2008;9:286–98.
[27] Nguyen L-T, Schmidt HA, von Haeseler A, Minh BQ. IQ-TREE: a fast and effective stochastic algorithm for estimating maximum-likelihood phylogenies. Mol Biol Evolut 2015;32:268–74.
[28] Sagulenko P, Puller V, Neher RA. TreeTime: Maximum-likelihood phylodynamic analysis. Virus Evolut 2018;4. doi: 10.1093/ve/vex042.
[29] Recurrent emergence and transmission of a SARS-CoV-2 Spike deletion ΔH69/V70 | bioRxiv. https://www.biorxiv.org/content/10.1101/2020.12.14.422555v3 (Accessed 26 December 2020).
[30] McCarthy KR, Rennick LJ, Nambulli S, et al. Recurrent deletions in the SARS-CoV-2 spike glycoprotein drive antibody escape. Science 2021;371:1139–42.
[31] Weisblum Y, Schmidt F, Zhang F, et al. Escape from neutralizing antibodies by SARS-CoV-2 spike protein variants. eLife 2020;9:e61312.
[32] Thomson EC, Rosen LE, Shepherd JG, et al. The circulating SARS-CoV-2 spike variant N439K maintains fitness while evading antibody-mediated immunity. Microbiology 2020. doi: 10.1101/2020.11.04.355842.
[33] Liu Z, VanBlargan LA, Rothlauf PW, et al. Landscape analysis of escape variants identifies SARS-CoV-2 spike mutations that attenuate monoclonal and serum antibody neutralization. bioRxiv 2020 2020.11.06.372037.
[34] Andreano E, Piccini G, Licastro D, et al. SARS-CoV-2 escape in vitro from a highly neutralizing COVID-19 convalescent plasma. bioRxiv 2020 2020.12.28.424451.
[35] Greaney AJ, Starr TN, Gilchuk P, et al. Complete mapping of mutations to the SARS-CoV-2 spike receptor-binding domain that escape antibody recognition. Cell Host Microbe 2021;29:44–57 e9.